SERBIAN JOURNAL OF ELECTRICAL ENGINEERING
Vol. 14, No. 2, June 2017, 199-216

UDC: 621.3 **DOI: https://doi.org/10.2298/SJEE161115002R**

Optimization of Electric and Magnetic Field Emissions Produced by Independent Parallel Overhead Power Lines

Aleksandar Ranković[1], Vladica Mijailović[1], Dimitrije Rozgić[1], Dragan Ćetenović[1]

Abstract: This paper presents a method for determining optimal arrangements of parallel independent overhead power lines aimed to decrease electric and magnetic field emissions. The Genetic Algorithm (GA) is used to find the optimal placement of conductors. The Monte Carlo approach implemented in GA allows consideration of uncertain phase shifts between independent overhead power lines. The results and practical aspects of the proposed methodology are illustrated on two different configurations of both independent 400 kV single-circuit and double-circuit overhead power lines.

Keywords: Magnetic field, Electric field, Phase shift, Genetic algorithm, Optimization.

1 Introduction

Potential implications for human health of low-frequency electric and magnetic fields (EMFs) have been looked at in a number of epidemiological studies (for overview, see [1]). Common sources of low-frequency EMFs include overhead power lines (OHPLs), electrical substations and electrical appliances. High values of EMFs have been reported especially at sites in close vicinity of high voltage OHPLs therefore the OHPLs should be designed in such manner so as to minimize electric and magnetic field emissions.

In the case of extremely low-frequency fields the electric field strength depends on voltage, while the magnetic field strength depends on the value of the electric current. Thus, by varying the current value, the magnetic field strength can be varied too. The international and national standards set both public and occupational limits based on short-term or long-term exposure of humans to the magnetic field [2] and its impact on human health. Short-term exposure of humans to magnetic field and its impact on their health relies on the conservative approach based on the worst-case scenario which involves the

[1]University of Kragujevac, Faculty of Technical Sciences Čačak, Serbia;
E-mails: aleksandar.rankovic@ftn.kg.ac.rs; vladica.mijailovic@ftn.kg.ac.rs; dimitrije.rozgic@ftn.kg.ac.rs; dragan.cetenovic@ftn.kg.ac.rs

maximum value of magnetic field, while long-term exposure of humans to magnetic field and its impact on health evaluates continuous exposure of humans to variable magnetic field in space and time.

Both the European Union and the Republic of Serbia have adopted limits only for short-term exposure to magnetic field [2, 3]. The worst-case scenario, for single-circuit OHPL, takes into consideration maximum values for lines current and conductor sag, while in double-circuit OHPL the same phase shift angle for both terns of phase conductors is the additional hypothesis [4]. The effects of rearranging the double-circuit phase succession and optimization methods used to solve problems of optimal arrangements of double-circuit OHPL intended to decrease electric and magnetic field emissions are the subject of numerous studies (for an overview see [5]).

In the worst-case scenario the phase shifts values are needed to optimize the arrangements of more than two independent OHPLs (single-circuit or double-circuit). Typically, information about the phase shift is not available in practice, especially for new OHPLs at the design stage. Therefore, each of the phase shifts can be treated as random variables uniformly distributed inside the interval. The huge number of possible phase shifts combination clearly disregards brute-force searching as a solution methodology.

In this paper, a novel method for determining optimal arrangements of independent parallel OHPLs aimed to decrease electric and magnetic field emissions is proposed. The Genetic Algorithm (GA) is used to find the optimal placement of conductors. The single-objective GA approach uses a weighted method to combine the two objectives (electric and magnetic field strengths) into a single objective function. The Monte Carlo simulations implemented in GA allow for the consideration of uncertain phase shifts between independent power lines and enable to finding the worst-case scenario. Literature provides only few recommendations for the sample size of Monte Carlo approach. In this paper, we examined the influence of sample size on the proposed optimization method.

This paper is arranged as follows. *Section* 2 describes the methodology for the calculation of high-voltage OHPLs electric and magnetic fields. *Section* 3 proposes hybrid Monte Carlo simulations/GA-based minimization procedure, described in detail. *Section* 4 presents results for two real-life test systems (from Electric Power Industry of Serbia). The concluding section summarizes the results obtained from the test systems.

2 Problem Formulation

In order to determine electric and magnetic fields it is necessary to solve coupled Maxwell's equations. In the quasi-static approximation of extremely

low-frequency fields, the Maxwell's equations become decoupled and electric and magnetic fields can be calculated separately.

2.1 Calculation of magnetic field of high-voltage overhead power lines

Fig. 1 shows a basic catenary geometry for a sagged conductor, where f_c is the conductor's sag.

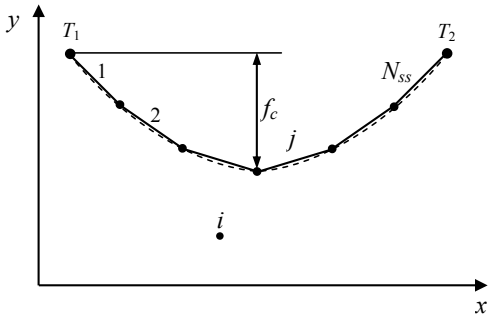

Fig. 1 – *Modeling of the sagged conductor (dashed line) with a finite number of straight segments (solid lines).*

A catenary of OHPL is described by equation [5]:

$$y = k_c \cosh\left(\frac{x}{k_c} + c_1\right) + c_2 , \tag{1}$$

where:

x, y – conductor coordinates;

k_c – parameter of the catenary (the ratio between the horizontal component of the conductor tensile force and the conductor weight per unit length);

c_1, c_2 – constants determined by the boundary conditions (defined from ending points of a conductor suspended between two towers).

Applying Biot-Savart law, the magnetic flux density vector in an observation point i is:

$$\vec{B} = \mu_0 \int_{l_c} \frac{I \, \mathrm{d}\vec{l} \times \vec{r}}{4\pi r^3} , \tag{2}$$

where:

μ_0 – the vacuum permeability;

l_c – the length of the conductor;

$\mathrm{d}\vec{l}$ – differential element at the direction of current;

$\vec{r}$ – vector whose magnitude r is the distance from the source to the observation point.

For the power line described by (1), the vectors of magnetic flux density and electric field strength in observation point cannot be determined analytically [6]. The magnetic field density components in *x*–, *y*– and *z*– directions in observation point i of one periodically sagged conductor divided on straight segments, shown as solid line in Fig. 1, can be calculated applying the superposition theorem:

$$B_{x(y,z)i} = \sum_{j=1}^{n} B_{x(y,z)ij}; \quad n = N_s N_{ss}, \tag{3}$$

where:

n – the number of observed straight segments;

$B_{x(y,z)ij}$ – components of the magnetic flux density of the straight segment in the *x*–, *y*– and *z*– directions, respectively;

i – total number of the observation points, $i = 1, 2, \cdots, N_p$;

N_s – the number of spans;

N_{ss} – the number of straight segments of the sagged conductor.

The effects of the currents induced in the earth on the total magnetic field produced under OHPLs can be modeled by a perfect conducting plane located at a complex depth below the earth surface [7]. If the radial distance from the conductor to the point of interest is substantially smaller than the penetration depth of image ground currents, the effect of the currents induced in the earth on the total magnetic field produced under the OHPLs is negligible [6]. Given that typical values of the penetration depth at 50 (60) Hz are 350 – 1600 m (for the earth resistivity lying in the range 50 – 1000 Ωm), the approximate formula (2) is valid for observation points under the OHPLs.

As for three-phase power lines, the line currents are sinusoidally varying with time at power frequency. For *K* three-phase balanced system, the *K* terns of current can be written as follows:

$$\begin{aligned} i_{a_k}(t) &= \sqrt{2} I_k \sin\left(\omega t + \varphi_k\right); \\ i_{b_k}(t) &= \sqrt{2} I_k \sin\left(\omega t + \varphi_k - 120°\right); \\ i_{c_k}(t) &= \sqrt{2} I_k \sin\left(\omega t + \varphi_k + 120°\right), \end{aligned} \tag{4}$$

where:

a, b, c – indices of phases conductor, respectively;

I_k – effective value of *k*-th tern of current;

k – number of terns, $k = 1, 2, \cdots, K$;

φ_k – phase shift of *k*-th tern of current.

Consequently, the magnetic field in the vicinity of the OHPLs also varies at the power frequency and can be made by superposition of the results calculated separately for each phase conductor given in (3). If the superposition theorem is applied and all phase conductors are taken into consideration, the obtained complex components of the magnetic flux density in observation point in *x*–, *y*– and *z*– directions can be written in matrix form as:

$$\underline{\boldsymbol{B}}_i(\boldsymbol{I},\varphi)=\boldsymbol{B}_i(\boldsymbol{I})\boldsymbol{e}(\varphi)\,, \tag{5}$$

where $\underline{\boldsymbol{B}}_i(\boldsymbol{I},\varphi)$ is three-dimensional complex vector of the magnetic flux density in observation point *i* in the *x*–, *y*– and *z*– directions:

$$\underline{\boldsymbol{B}}_i(\boldsymbol{I},\varphi)=\left[\underline{\boldsymbol{B}}_{xi}\;\;\underline{\boldsymbol{B}}_{yi}\;\;\underline{\boldsymbol{B}}_{zi}\right]^T, \tag{6}$$

$\boldsymbol{B}_i(\boldsymbol{I})$ is a matrix of the magnetic flux density of each phase conductor in observation point *i* in the *x*–, *y*– and *z*– directions, respectively:

$$\boldsymbol{B}_i(\boldsymbol{I})=\begin{bmatrix} B_{xi}^{a_1}(I_1) & B_{xi}^{b_1}(I_1) & B_{xi}^{c_1}(I_1) & \cdots & B_{xi}^{a_k}(I_k) & B_{xi}^{b_k}(I_k) & B_{xi}^{c_k}(I_k) & \cdots & B_{xi}^{a_K}(I_K) & B_{xi}^{b_K}(I_K) & B_{xi}^{c_K}(I_K) \\ B_{yi}^{a_1}(I_1) & B_{yi}^{b_1}(I_1) & B_{yi}^{c_1}(I_1) & \cdots & B_{yi}^{a_k}(I_k) & B_{yi}^{b_k}(I_k) & B_{yi}^{c_k}(I_k) & \cdots & B_{yi}^{a_K}(I_K) & B_{yi}^{b_K}(I_K) & B_{yi}^{c_K}(I_K) \\ B_{zi}^{a_1}(I_1) & B_{zi}^{b_1}(I_1) & B_{zi}^{c_1}(I_1) & \cdots & B_{zi}^{a_k}(I_k) & B_{zi}^{b_k}(I_k) & B_{zi}^{c_k}(I_k) & \cdots & B_{zi}^{a_K}(I_K) & B_{zi}^{b_K}(I_K) & B_{zi}^{c_K}(I_K) \end{bmatrix} \tag{7}$$

and $\boldsymbol{e}(\varphi)$ is a 3*K*-dimensional complex vector:

$$\boldsymbol{e}(\varphi)=\left[\mathrm{e}^{\mathrm{j}\varphi_1}\;\;\mathrm{e}^{\mathrm{j}(\varphi_1-120°)}\;\;\mathrm{e}^{\mathrm{j}(\varphi_1+120°)}\;\cdots\;\mathrm{e}^{\mathrm{j}\varphi_k}\;\;\mathrm{e}^{\mathrm{j}(\varphi_k-120°)}\;\;\mathrm{e}^{\mathrm{j}(\varphi_k+120°)}\;\cdots\;\mathrm{e}^{\mathrm{j}\varphi_K}\;\;\mathrm{e}^{\mathrm{j}(\varphi_K-120°)}\;\;\mathrm{e}^{\mathrm{j}(\varphi_K+120°)}\right]^T. \tag{8}$$

The effective values of current and phase shift of all terns can be given in vector form:

$$\boldsymbol{I}=\left[I_1\;\;\cdots\;\;I_k\;\;\cdots\;\;I_K\right]^T, \tag{9}$$

$$\varphi=\left[\varphi_1\;\;\cdots\;\;\varphi_k\;\;\cdots\;\;\varphi_K\right]^T. \tag{10}$$

Effective value of the magnetic flux density (root mean square value) is [5]:

$$B_i=\sqrt{\left|\underline{B}_{xi}\right|^2+\left|\underline{B}_{yi}\right|^2+\left|\underline{B}_{zi}\right|^2}\,. \tag{11}$$

2.2 Calculation of electric field of high-voltage overhead power lines

To determine the three-dimensional electric field distribution near transmission lines, a numerical calculation based on Charge Simulation Method (CSM) is proposed [8]. The phase conductors and ground wires are represented by the line charges. For a representation of non-uniform surface charge distribution, the phase conductors and ground wires described by the catenary equation is subdivided into straight segments with unknown fictitious complex linear charge, as shown in Fig 1. Simulation linear charges are set in the centre

of each straight segment therefore boundary conditions are satisfied in some matching points on the conductor surface. Potential errors exist in all other conductor surface positions. The influence of earth surface is replaced with the images of conductors located at a depth equal to the conductor's height, applying the image theorem.

In order to determine n_c unknown fictitious complex linear charge used to simulate the surface charge distribution of transmission lines, the same numbers of testing points on the surface of conductor are selected. The potential at this contour point is equal to the conductor's potential. The potentials of the testing points can be calculated by superposition of fictitious line charges:

$$\underline{\boldsymbol{V}} = \boldsymbol{P} \cdot \underline{\boldsymbol{Q}}, \tag{12}$$

where:

$\boldsymbol{P}$ – the matrix of potential coefficient of the observed straight segments;

$\boldsymbol{Q}$ – vector of unknown fictitious complex linear charge;

$\boldsymbol{V}$ – the vector of known potentials in the contour points of phase conductors and ground wires.

The fictitious complex linear charge can be determined by matrix inversion:

$$\underline{\boldsymbol{Q}} = \boldsymbol{P}^{-1} \cdot \underline{\boldsymbol{V}}. \tag{13}$$

The electric field strength components in x–, y– and z– directions in observation point i of the air space are a superposition of electric field produced by the fictitious complex linear charge:

$$E_{x\,(y,\,z)i} = \sum_{j=1}^{n_c} E_{x\,(y,\,z)ij} = \sum_{j=1}^{n_c} F_{x\,(y,\,z)ij} \cdot \underline{Q}_j \ . \tag{14}$$

The components of the electric field strength coefficient of the straight segment and their images in the x–, y– and z– directions are [5]:

$$F_{x\,(y,\,z)ij} = -\frac{\partial P_{ij}}{\partial x\,(y,\,z)_i}. \tag{15}$$

For the K three-phase balanced system, the K terns of phase voltage can be written as follows:

$$\begin{aligned} v_{a_k}(t) &= \sqrt{2} V_k \sin\left(\omega t + \theta_k\right); \\ v_{b_k}(t) &= \sqrt{2} V_k \sin\left(\omega t + \theta_k - 120°\right); \\ v_{c_k}(t) &= \sqrt{2} V_k \sin\left(\omega t + \theta_k + 120°\right), \end{aligned} \tag{16}$$

where:

V_k – effective value of k-th tern of phase voltage and

θ_k – phase shift of k-th tern of phase voltage.

By analogy with methodology for calculation of complex components of the magnetic flux density, the obtained complex components of the electric field strength in observation point in *x*-, *y*- and *z*- directions can be written in matrix form as:

$$\underline{\boldsymbol{E}}_i(\boldsymbol{V},\boldsymbol{\theta}) = \boldsymbol{E}_i(\boldsymbol{V})\cdot\boldsymbol{e}(\boldsymbol{\theta}), \tag{17}$$

where $\boldsymbol{E}_i(\boldsymbol{V})$ is a matrix of the electric field strength of each phase conductor in observation point *i* in the *x*-, *y*- and *z*- directions, respectively:

$$\boldsymbol{E}_i(\boldsymbol{V})=\begin{bmatrix} E_{xi}^{a_1}(V_1) & E_{xi}^{b_1}(V_1) & E_{xi}^{c_1}(V_1) \cdots E_{xi}^{a_k}(V_k) & E_{xi}^{b_k}(V_k) & E_{xi}^{c_k}(V_k) \cdots E_{xi}^{a_K}(V_K) & E_{xi}^{b_K}(V_K) & E_{xi}^{c_K}(V_K) \\ E_{yi}^{a_1}(V_1) & E_{yi}^{b_1}(V_1) & E_{yi}^{c_1}(V_1) \cdots E_{yi}^{a_k}(V_k) & E_{yi}^{b_k}(V_k) & E_{yi}^{c_k}(V_k) \cdots E_{yi}^{a_K}(V_K) & E_{yi}^{b_K}(V_K) & E_{yi}^{c_K}(V_K) \\ E_{zi}^{a_1}(V_1) & E_{zi}^{b_1}(V_1) & E_{zi}^{c_1}(V_1) \cdots E_{zi}^{a_k}(V_k) & E_{zi}^{b_k}(V_k) & E_{zi}^{c_k}(V_k) \cdots E_{zi}^{a_K}(V_K) & E_{zi}^{b_K}(V_K) & E_{zi}^{c_K}(V_K) \end{bmatrix} \tag{18}$$

and $\boldsymbol{e}(\boldsymbol{\theta})$ is a 3*K*-dimensional complex vector:

$$\boldsymbol{e}(\boldsymbol{\theta}) = \left[\mathrm{e}^{\mathrm{j}\theta_1} \quad \mathrm{e}^{\mathrm{j}(\theta_1-120°)} \quad \mathrm{e}^{\mathrm{j}(\theta_1+120°)} \cdots \mathrm{e}^{\mathrm{j}\theta_k} \quad \mathrm{e}^{\mathrm{j}(\theta_k-120°)} \quad \mathrm{e}^{\mathrm{j}(\theta_k+120°)} \cdots \mathrm{e}^{\mathrm{j}\theta_K} \quad \mathrm{e}^{\mathrm{j}(\theta_K-120°)} \quad \mathrm{e}^{\mathrm{j}(\theta_K+120°)} \right]^T. \tag{19}$$

The effective values of phase voltage and phase shift of all terns can be given in vector form:

$$\boldsymbol{V} = \left[V_1 \quad \cdots \quad V_k \quad \cdots \quad V_K \right]^T, \tag{20}$$

$$\boldsymbol{\theta} = \left[\theta_1 \quad \cdots \quad \theta_k \quad \cdots \quad \theta_K \right]^T. \tag{21}$$

Effective value of the electric field strength is:

$$E_i = \sqrt{\left|\underline{E}_{xi}\right|^2 + \left|\underline{E}_{yi}\right|^2 + \left|\underline{E}_{zi}\right|^2}. \tag{22}$$

Observe that the phase shift of tern 1 is assumed as the reference and it is assigned the value of $\varphi_1 = 0°$ and $\theta_1 = 0°$.

3 Optimization Procedure

The multiple-objective optimization technique, proposed in this paper, uses the trade-off information in the form of weights to measure the relative importance of different objective functions. These weights can also be interpreted as rating coefficients attached to the unit values of the different objective functions. This optimization method combines two conflicting objectives into a single fitness function. The result of this approach is the single best solution of optimization.

A single-objective problem is defined, which seeks to minimize the magnetic flux density and electric field strength. The methods used to calculate magnetic flux density and electric field strength are briefly described in

Section 2. Both objective functions are considered to be equally important and normalized by rating coefficients (limit values of magnetic flux density and electric field strength). The single-objective optimization function is formulated as [9]:

$$f_{B,E}(\boldsymbol{y}, \boldsymbol{z}, \boldsymbol{\varphi}_{MC}, \boldsymbol{\theta}_{MC}) = \left(\frac{B(\boldsymbol{y}, \boldsymbol{z}, \boldsymbol{\varphi}_{MC})}{\sqrt{2}B_U} \right)^2 + \left(\frac{E(\boldsymbol{y}, \boldsymbol{z}, \boldsymbol{\theta}_{MC})}{\sqrt{2}E_U} \right)^2, \tag{23}$$

subject to: $g_m(\boldsymbol{y}, \boldsymbol{z}) \le 0; \quad m = 1, 2, \cdots, M$;

$$y_n^{(L)} \le y_n \le y_n^{(U)}, \quad z_n^{(L)} \le z_n \le z_n^{(U)}; \quad n = 1, 2, \cdots, N,$$

where:

$\boldsymbol{y}, \boldsymbol{z}$ – the decision variable vectors (heights of conductor attachment point and conductor distance orthogonally to the line direction, respectively);

$\boldsymbol{\varphi}_{MC}, \boldsymbol{\theta}_{MC}$ – matrices of current and voltage phase shift vectors samples, respectively;

B_U, E_U – the magnetic flux density and electric field strength limit values, respectively;

$g_m(\boldsymbol{y}, \boldsymbol{z})$ – the inequality constraints;

M – the number of inequality constraints;

$y_{n,}^{(L)}$ $y_{n,}^{(U)}$ $z_{n,}^{(L)}$ $z_n^{(U)}$ – lower and upper limits of decision variables;

N – the number of all conductors.

The inequality constraints $g_m(\boldsymbol{y}, \boldsymbol{z})$ are defined to satisfy the predefined values of [5]:

– The minimum distance between phase conductors C_{pp}, and the minimum distance between phase conductor and object at the earth potential C_{el};

– The minimal earth-wire conductor height H_{ew} subject to satisfy the shielding angle.

The minimum distance C_{pp} and C_{el} are, respectively [9]:

$$C_{pp} = k\sqrt{f_c + l_k} + K_1 D_{pp}, \tag{24}$$

$$C_{el} = k\sqrt{f_c + l_k} + K_1 D_{el}, \tag{25}$$

where:

k – the factor depending on relative position of two conductors and the swing angle of conductor caused by wind;

f_c – the sag of conductor, in [m];

l_k – the length of insulator set swinging orthogonally to the line direction, in [m];

K_1 – the reduction factor for electrical clearances,

D_{pp}, D_{el} – minimum air clearances between phase conductors, and phase conductor and object at earth potential, respectively.

Minimum air clearances are established based on lightning, switching surge or power frequency considerations. The details of the calculation of the minimum distances and minimum air clearances are given in [5, 10–12].

In order to examine maximum exposure-scenario of magnetic flux density and electric field strength, the maximum value of phase current and maximum sag of conductor are adopted. Also, the phase shifts of phase currents and voltage are treated as random variables uniformly distributed inside the interval: $\varphi_{\min} \le \varphi \le \varphi_{\max}$ and $\theta_{\min} \le \theta \le \theta_{\max}$, respectively [13].

In this paper hybrid Monte Carlo simulations/GA based minimization procedure can be implemented to minimize value of EMF strengths. GA is used to minimize the single-objective optimization function $f_{B,E}(\boldsymbol{y}, \boldsymbol{z}, \boldsymbol{\varphi}_{MC}, \boldsymbol{\theta}_{MC})$ and identify the best position of the conductors. To figure out maximum value of magnetic flux density and electric field strength for the worst-case phase shift scenario, Monte Carlo simulations are introduced into each GA steps. For each position of conductors $(\boldsymbol{y}, \boldsymbol{z})$ generated by GA, Monte Carlo simulations generates random phase shift vectors and identifies maximum value of magnetic induction and electric field across all observation points *i*:

$$B(\boldsymbol{y}, \boldsymbol{z}, \boldsymbol{\varphi}_{MC}) = \max_{l,i} \left\{ B_i(\boldsymbol{y}, \boldsymbol{z}, \boldsymbol{\varphi}_l) \right\}; \quad l = 1, 2, \cdots, L, \tag{26}$$

$$E(\boldsymbol{y}, \boldsymbol{z}, \boldsymbol{\theta}_{MC}) = \max_{l,i} \left\{ E_i(\boldsymbol{y}, \boldsymbol{z}, \boldsymbol{\theta}_l) \right\}; \quad l = 1, 2, \cdots, L, \tag{27}$$

where L independent random samples of phase shift vectors $\boldsymbol{\varphi}_l$ and $\boldsymbol{\theta}_l$ of length K (see eqs. (10) and (21)) can be written in the matrix form:

$$\boldsymbol{\varphi}_{MC} = \begin{bmatrix} \varphi_{11} & \cdots & \varphi_{1l} & \cdots & \varphi_{1L} \\ \vdots & \ddots & \vdots & & \vdots \\ \varphi_{k1} & \cdots & \varphi_{kl} & \cdots & \varphi_{kL} \\ \vdots & & \vdots & \ddots & \vdots \\ \varphi_{K1} & \cdots & \varphi_{Kl} & \cdots & \varphi_{KL} \end{bmatrix} = \begin{bmatrix} \boldsymbol{\varphi}_1 & \cdots & \boldsymbol{\varphi}_l & \cdots & \boldsymbol{\varphi}_L \end{bmatrix}, \tag{28}$$

$$\boldsymbol{\theta}_{MC} = \begin{bmatrix} \boldsymbol{\theta}_1 & \cdots & \boldsymbol{\theta}_l & \cdots & \boldsymbol{\theta}_L \end{bmatrix}. \tag{29}$$

It is to be observed that to repeat Monte Carlo simulations with same conditions into each GA steps we use identical collection of random phase shift vectors $\boldsymbol{\varphi}_{MC}$ and $\boldsymbol{\theta}_{MC}$. The proposed iterative scheme for determining optimal arrangements of independent OHPLs is shown as flow-chart in Fig. 2.

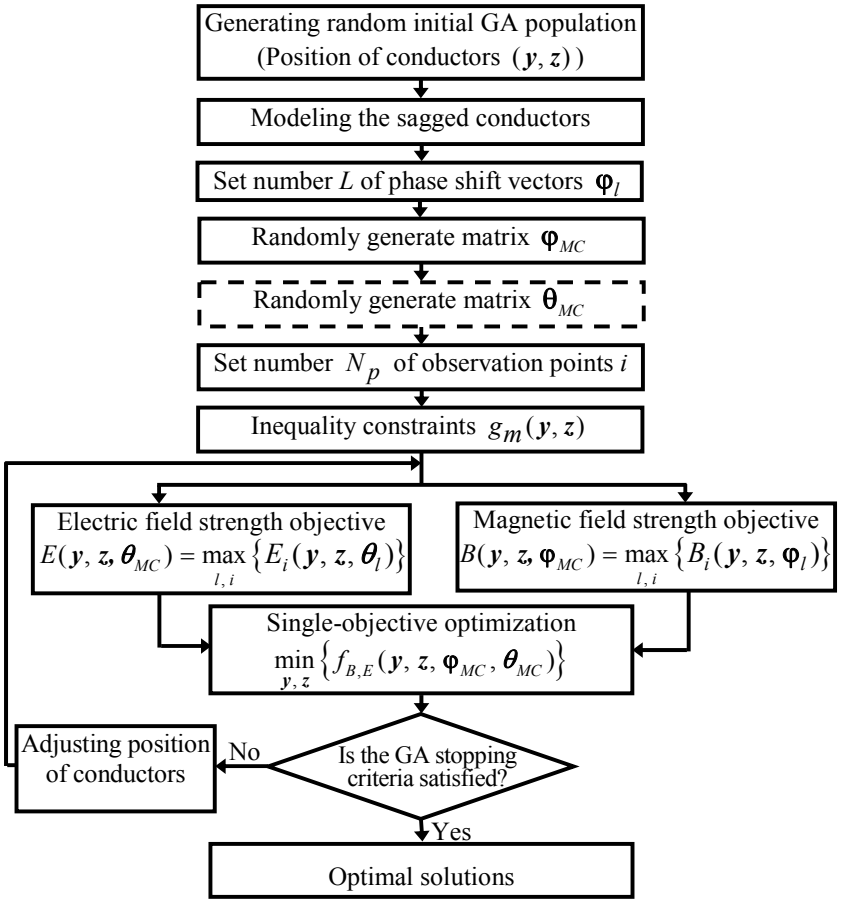

Fig. 2 – *Flow chart of the proposed iterative scheme for determining optimal arrangements of independent OHPLs.*

Randomly generated matrix of phase shift vectors $\boldsymbol{\theta}_{MC}$.(denoted as dashed lines box in Fig.2) is used only specifically when the power line is equipped with a phase shifting transformer (PST). PSTs, also known as phase angle regulators or quadrature boosters, are special transformers used to control power flows in transmission networks creating a phase shift between the beginning and the ending terminals of the power line [14]. For transmission line without PST, randomly generated matrix of phase shift vectors $\boldsymbol{\theta}_{MC}$ is reduced into null vector.

The GA convergence criterion is that there are not changes in decision variables (position of conductors) of single-objective optimization function (see (23)) in two subsequent GA generations.

4 Numerical Results

The proposed method for determining optimal arrangements of independent OHPLs is applied to two different configurations:

- One double-circuit and one single-circuit parallel 400 kV OHPLs;
- Two double-circuit parallel 400 kV OHPLs.

Optimal arrangements of independent OHPLs for the configurations proposed above are analyzed under the two different scenarios:

- OHPLs carry electric power from generating plants to the substations operated at a high ratio of real power to the reactive power, with power factor higher than 0.8 lagging (phase shifts of phase current are uniformly distributed inside the interval: $0° \le \varphi \le 36.86°$), denoted as Scenario 1;
- Real power and reactive power of independent OHPLs may flow in both directions and the phase-shift angle can vary over the whole theoretical range: $0° \le \varphi \le 360°$ [4, 15], denoted as Scenario 2.

It is to be observed that all OHPLs used in Electric Power Industry of Serbia Company are not equipped with a PST, thus the phase shift vector θ_{MC} is reduced to null vector for the both scenarios proposed.

4.1 One double-circuit and one single-circuit parallel 400 kV overhead power lines

In the analyzed test example, three terns, one double-circuit OHPL with a single earth-wire and single-circuit horizontal 400 kV OHPL with two earth-wires are presented. The distance between the axis of the first and second OHPL is 30 m (denoted as vertical dashed lines in Figs. 4 and 5). The data of OHPLs are given in **Table 1**. The influence of five identical spans with equal heights of the beginning and ending points is observed. Each span of the sagged subconductor is approximated with six straight segments.

Table 1

Data of 400 kV double-circuit and single-circuit OHPL.

Span length [m]	300
Number of subconductors in the bundle	2
Diameter of subconductors [mm]	30.6
Distance between subconductors [cm]	40
Subconductors sag [m]	7.0
Diameter of earth-wire [mm]	9.0
Earth-wire sag [m]	3.5
Phase current [A]	1500

Magnetic flux density and electric field strength are calculated at the mid span along the lateral profile, 1 m above the ground and optimum phase conductor succession ($a_{11}b_{11}c_{11}\ c_{12}b_{12}a_{12}$ for double-circuit OHPL and $a_2b_2c_2$ for single-circuit OHPL) for EMF strengths minimization [16].

The genetic search is performed with a population size of 60 members, the crossover and mutation rates being 0.8 and 0.01, respectively. The values of GA parameters, which represent the trade-off between the desired solution efficiency and their predictive accuracy, were determined upon several experiments. The adopted limit values $B_U = 40\,\mu\text{T}$ and $E_U = 2\,\text{kV/m}$ represent the maximum national quantitative limits of exposure of the general public to electromagnetic fields in Republic of Serbia [3].

Given the symmetrical arrangements of phase conductors in our test example (one double-circuit power line with one earth-wire, and single-circuit horizontal power line with two earth-wire), the position of conductors are defined with eleven decision variables grouped into two decision variable vectors:

$$\begin{aligned} \boldsymbol{y} &= \left[y_{a_{12}} \quad y_{b_{12}} \quad y_{c_{12}} \quad y_{ew_1} \quad y_{a_2} \quad y_{ew_{21}} \right]; \\ \boldsymbol{z} &= \left[z_{a_{12}} \quad z_{b_{12}} \quad z_{c_{12}} \quad z_{a_2} \quad z_{ew_{21}} \right]. \end{aligned} \tag{29}$$

The calculated phase-to-phase minimum distance is $C_{pp} = 7\,\text{m}$, whereas the minimum distance of conductor to the tower body is $C_{el} = 3.55\,\text{m}$ [5]. The minimal heights of earth-wire conductors are calculated to provide a shield angle of 30^{o} which is defined by the standard.

In order to investigate the uncertainty impact on the proposed optimization GA algorithm, in Monte Carlo simulations the phase shifts of two terns (φ_2 and φ_3) are varied and analyzed in four characteristic numbers of L independent random samples of phase shift vectors $\boldsymbol{\varphi}_l$, i.e. 100, 1000, 5000 and 10000. The proposed sensitivity analysis is used to determine whether or not the model responds in the expected way to the changes of numbers of L independent samples.

The results of the optimization are compared with the initial conductor arrangements (existing, unoptimized lines). The initial and optimized conductor arrangements of one double-circuit and one single-circuit parallel 400 kV OHPLs are shown in Fig. 3 for both cases analyzed. One tern of double-circuit power line ($a_{11}b_{11}c_{11}$) is omitted from Fig. 3 because of the conductor symmetry. Also, one symbol in Fig. 3 represents the center of the bundle.

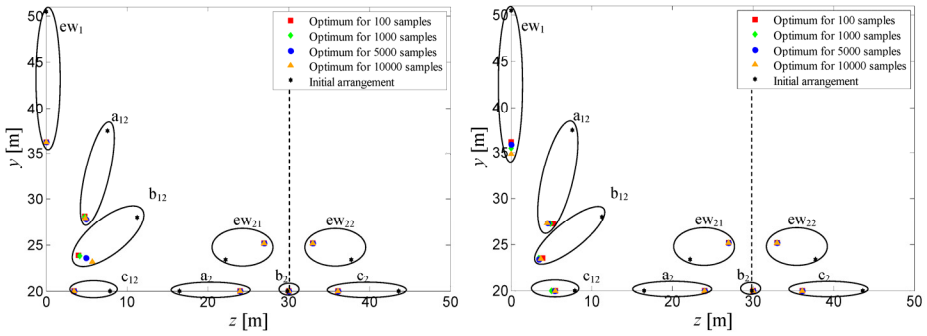

a) *Scenario* 1 b) *Scenario* 2

Fig. 3 – *Initial and optimized conductor arrangements of one single-circuit and one double-circuit parallel 400 kV OHPLs, for both analyzed scenarios.*

Fig. 3 shows that the optimization of the conductor arrangements significantly reduces size of the tower.

The influence of phase shift on magnetic field of the existing line is examined in two cases:

- Maximum value of magnetic flux density is determined when phase shift of all terns is of the same value. We assign 0° value, denoted as *Initial arrangement - neglected phase shift* case;
- Maximum value of magnetic flux density is determined for the worst-case phase shift scenario using Monte Carlo simulation (see (26)), denoted as *Initial arrangement - included phase shift* case.

Figs. 4 and 5 show the comparison between the lateral magnetic flux density and electric field strength profiles under one double-circuit and one single-circuit parallel 400 kV OHPLs at the mid span calculated for initial and optimized conductor arrangements.

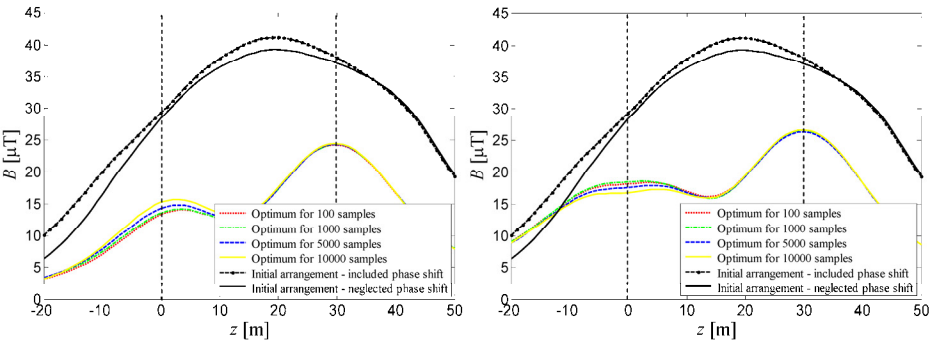

a) *Scenario* 1 b) *Scenario* 2

Fig. 4 – *The lateral magnetic flux density profiles under one double-circuit and one single-circuit parallel 400 kV OHPLs at the mid span.*

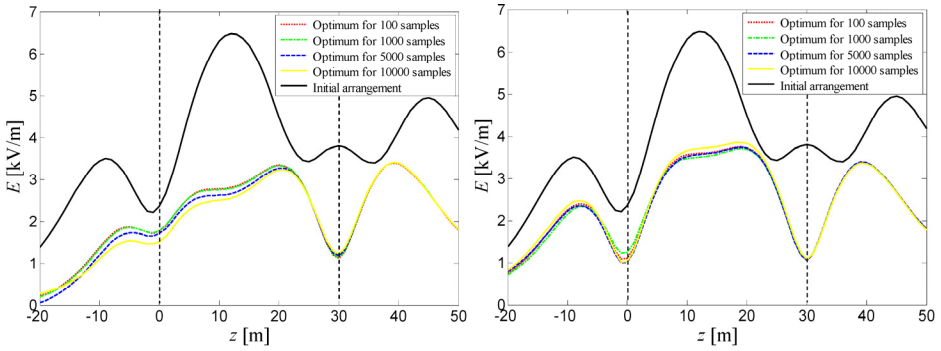

a) *Scenario* 1 b) *Scenario* 2

Fig. 5 – *The lateral electric field strength profiles under (a) one double-circuit and (b) one single-circuit parallel 400 kV OHPLs at the mid span.*

The obtained results of sensitivity analysis for two previously proposed scenarios are shown in **Table 2**.

Table 2

Comparison between the initial and optimized conductor arrangements, for both analyzed scenarios.

		OPTIMIZED ARRANGEMENT				INITIAL ARRANGEMENT	
		Numbers of phase shifts samples				Included phase shift	Neglected phase shift
		100	1000	5000	10000		
Scenario 1	Phase shift φ_2 (°)	34.89	35.55	35.95	35.96	35.96	0
	Phase shift φ_3 (°)	5.83	1.08	0.98	0.78	8.20	0
	Maximum of magnetic flux density B_{max} (μT)	24.24	24.30	24.33	24.41	41.18	39.28
	Maximum of electric field strength E_{max} (kV)	3.41	3.42	3.42	3.42	6.48	
Scenario 2	Phase shift φ_2 (°)	198.04	184.76	181.41	177.84	213.84	0
	Phase shift φ_3 (°)	13.17	1.08	1.04	1.01	21.81	0
	Maximum of magnetic flux density B_{max} (μT)	26.34	26.55	26.58	26.60	44.92	39.28
	Maximum of electric field strength E_{max} (kV)	3.72	3.75	3.76	3.86	6.48	

The results presenting in Fig. 4 and **Table 2** show that phase shift has significant influence on maximum value of magnetic flux density.

The proposed optimization procedure reduces maximum of electric field strength and magnetic flux density between 40% and 50% as compared to the initial arrangement however maximum of electric field strength is still higher than adopted limit value. An alternative way of reducing electric field strengths is using higher OHPL tower or increasing the distance between OHPLs. Additionally, the results of sensitivity analysis show that optimization procedure with small sample size ($L = 100$) results in deviation of optimal arrangement of conductors (shown in Fig. 3) and phase shift values, given in **Table 2**. This deviation can be accounted for by the fact that a relatively small number of samples are not enough to meet normal distribution.

It is to be observed that increasing the sample size from 100 to more than 1000 only reduces the deviation of optimal arrangement of conductors, phase shift values, lateral magnetic flux density and electric field strength profiles, but does not make any noticeable improvements in results for maximum value of magnetic flux density and electric field strength.

4.2 Two double-circuit parallel 400 kV overhead power lines

The second test example deals with two identical double-circuit parallel 400 kV OHPLs with four independent terns. The parameters of OHPLs are set to the same values as given in *Section* 4.1. Considering the symmetrical arrangements of conductors for two identical double-circuit power lines, the positions of conductors are defined using seven decision variables grouped into two decision-variable vectors:

$$\begin{aligned} \boldsymbol{y} &= \left[y_{a_{12}} \quad y_{b_{12}} \quad y_{c_{12}} \quad y_{ew_1} \right]; \\ \boldsymbol{z} &= \left[z_{a_{12}} \quad z_{b_{12}} \quad z_{c_{12}} \right]. \end{aligned} \tag{30}$$

Also, the genetic search is performed with the same GA parameters values as given in *Section* 4.1.

However, when considering the worst-case phase shift scenario using Monte Carlo simulation it is worth observing that the increase in the number of terns results in the increase in the number of possible phase shift combinations. Therefore, in the test system analyzed, the phase shifts of three terns (φ_2 , φ_3 and φ_4) are varied and the numbers of L independent samples of phase shift vectors $\boldsymbol{\varphi}_l$ are increased (1000, 5000, 10000 and 20000).

Fig. 6 presents the existing and the optimized conductor arrangements. Because of the symmetry only one tern of first double-circuit power line ($a_{12}b_{12}c_{12}$) is showed in Fig. 6.

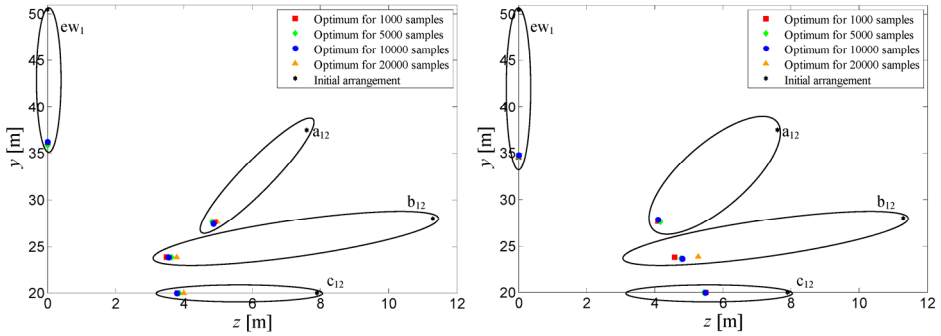

a) *Scenario* 1 b) *Scenario* 2

Fig. 6 – *Initial and optimized conductor arrangements of two double-circuit parallel 400 kV OHPLs, for both analyzed scenarios.*

The calculated magnetic flux density and electric field strength profiles are shown in Figs. 7 and 8. Both are given for the existing and the optimized conductor arrangements.

The obtained results in Fig. 7 confirm high influence of the phase shifts on magnetic flux density. For the both proposed scenarios and *Initial arrangement - neglected phase shift* case the maximum magnetic flux density is 17.73 μT, while the corresponding values for *Initial arrangement - included phase shift* case are 19.25 and 36.27 μT, respectively.

Additionally, the number of samples has a higher influence on optimization results compared with the test example given in *Section* 4.1. If this number is small, then lateral magnetic flux density and electric field strength profiles deviants from the results found at 20000 samples (see Figs. 7 and 8).

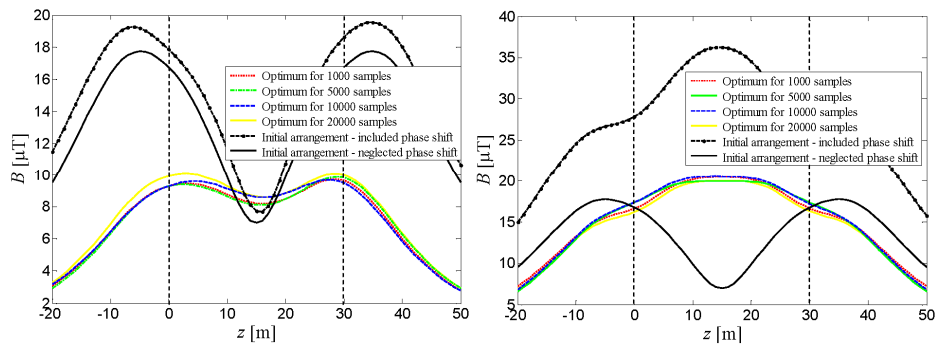

a) *Scenario* 1 b) *Scenario* 2

Fig. 7 – *Lateral magnetic flux density profiles under two double-circuit parallel 400 kV OHPLs at the mid span.*

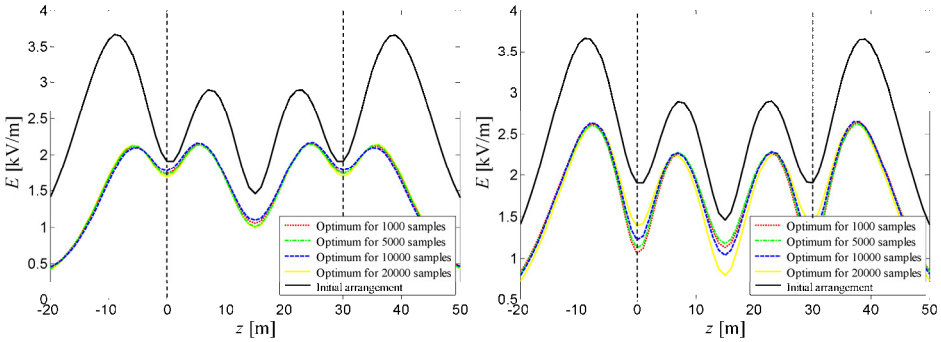

a) *Scenario* 1 b) *Scenario* 2

Fig. 8 – *Lateral electric field strength profiles under two double-circuit parallel 400 kV OHPLs at the mid span.*

5 Conclusion

The objective of this work is to propose methodology suitable for minimizing maximum value of electric and magnetic field emissions near independent overhead power lines. The proposed methodology explores the search space of solutions using hybrid Monte Carlo simulations/GA based minimization procedure to find the optimal placement of conductors.

Specifically, we showed how Monte Carlo approach can be useful for considering uncertain phase shifts between independent power lines and determining the worst-case scenario. Adequate numbers of phase shifts samples were introduced to enhance the efficacy of the proposed optimization method. The influence of phase shifts on optimal arrangements of independent overhead power lines has been confirmed in all the cases analyzed.

The proposed optimization method was successfully validated as a suitable approach for determining optimal arrangements of any conventional independent overhead power lines aimed at decreasing electric and magnetic field emissions.

6 Acknowledgement

The authors hereby express their sincere gratitude to the Ministry of Education and Science of the Republic of Serbia for their support to this work provided within projects III-42009.

7 References

[1] I.C. Ahlbom, E. Cardis, A. Green, M. Linet, D. Savitz, A. Swerdlow: Review of the Epidemiologic Literature on EMF and Health, Environmental Health Perspectives Supplements, Vol. 109, Supplement 6, Dec. 2001, pp. 911 – 933.

[2] EMS Info: Power-frequency EMF Exposure Standards Applicable in Europe and Elsewhere. Available at: http://www.emfs.info/wp-content/uploads/2015/07/standards-table-1-July-2015.pdf.

[3] Regulation on the Limits Exposure of Non-ionizing Radiation, Official Gazette of the Republic of Serbia, No. 104/09, Dec. 2009. (In Serbian).

[4] G. Mazzanti: The Role Played by Current Phase Shift on Magnetic Field Established by Double-circuit Overhead Transmission Lines - Part I: Static Analysis, IEEE Transaction on Power Delivery, Vol. 21, No. 2, April 2006, pp. 939 – 948.

[5] A. Ranković: Novel Multi-objective Optimization Method of Electric and Magnetic Field Emissions from Double-circuit Overhead Power Line, International Transactions on Electrical Energy Systems, Vol. 27, No. 2, Feb. 2017, p. e2243.

[6] K. Budnik, W. Machczyński: Contribution to Studies on Calculation of the Magnetic Field under Power Lines, European Transactions on Electrical Power, Vol. 16, No. 4, July/Aug. 2006, pp. 345 – 364.

[7] A.V. Mamishev, R.D. Nevels, B.D. Russell: Effects of Conductor Sag on Spatial Distribution of Power Line Magnetic Field, IEEE Transaction on Power Delivery, Vol. 11, No. 3, July 1996, pp. 1571 – 1576.

[8] N.H. Malik: A Review of Charge Simulation Method and its Application, IEEE Transactions on Electrical Insulation, Vol. 24, No. 1, Feb. 1989, pp. 3 – 20.

[9] K. Deželak, F. Jakl, G. Štumberger: Arrangements of Overhead Power Line Phase Conductors obtained by Differential Evolution, Electric Power Systems Research, Vol. 81, No. 12, Dec. 2011, pp. 2164 – 2170.

[10] F. Kiessling, P. Nefzger, J.F. Nolasco, U. Kaintzyk: Overhead Power Lines: Planning, Design, Construction, Springer, Berlin, Germany, 2003.

[11] IEC 60071-1 Edition 8.0: Insulation Coordination - Part 1: Definitions, Principles and Rules, Geneva, Switzerland, Jan. 2006.

[12] IEC 60071-2 Edition 3.0: Insulation Co-ordination - Part 2: Application Guide, Geneva, Switzerland, Dec. 1996.

[13] G. Lucca: Montecarlo Evaluation of Long Term Exposure to ELF Magnetic Field from Independent Power Lines, International Conference on Electromagnetic Fields Health and Environment, Wroclaw, Poland, 10-12 Sept. 2007, pp. 188 – 197.

[14] IEC 62032/IEEE C57.135 Edition 2.0: Guide for the Application, Specification, and Testing of Phase Shifting Transformers, Geneva, Switzerland, June 2012.

[15] G. Mazzanti: The Role Played by Current Phase Shift on Magnetic Field Established by Double-circuit Overhead Transmission Lines - Part II: Dynamic Analysis, IEEE Transaction on Power Delivery, Vol. 21, No. 2, April 2006, pp. 949 – 958.

[16] D. Tsanakas, J. Filippopoulos, J. Voyatzakis, G. Kouvarakis: Compact and Optimum Phase Conductor Arrangement for the Reduction of Electric and Magnetic Fields of Overhead Lines, CIGRE, Paris, France, 2000, Report No. 36-103.